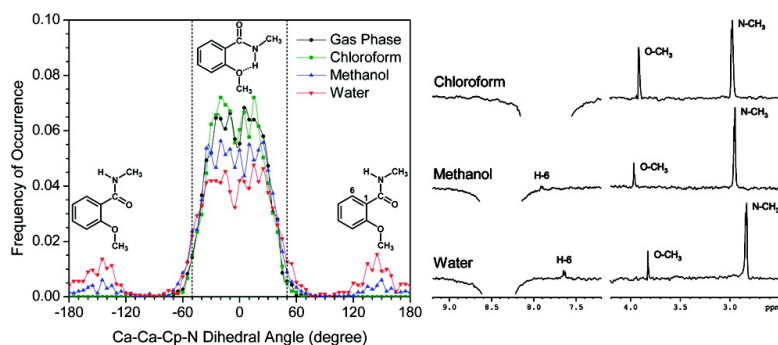


## Hydrogen Bonding in *ortho*-Substituted Arylamides: The Influence of Protic Solvents

Zhiwei Liu, Richard C. Remsing, Dahui Liu, Guillermo Moyna, and Vojislava Pophristic

*J. Phys. Chem. B*, **2009**, 113 (20), 7041-7044 • Publication Date (Web): 27 April 2009

Downloaded from <http://pubs.acs.org> on May 14, 2009



### More About This Article

Additional resources and features associated with this article are available within the HTML version:

- Supporting Information
- Access to high resolution figures
- Links to articles and content related to this article
- Copyright permission to reproduce figures and/or text from this article

[View the Full Text HTML](#)



ACS Publications  
High quality. High impact.

## Hydrogen Bonding in *ortho*-Substituted Arylamides: The Influence of Protic Solvents

Zhiwei Liu,<sup>†</sup> Richard C. Remsing,<sup>†</sup> Dahui Liu,<sup>‡</sup> Guillermo Moyna,<sup>†</sup> and Vojislava Pophristic<sup>\*,†</sup>

Department of Chemistry & Biochemistry and Center for Drug Design and Delivery, University of the Sciences in Philadelphia, 600 South 43rd Street, Philadelphia, Pennsylvania 19104-4495, and Polymedix Inc., 170 North Radnor Chester Road Suite 300, Radnor, Pennsylvania 19087-5280

Received: March 10, 2009; Revised Manuscript Received: April 8, 2009

We combine molecular modeling and NMR methods to better understand intramolecular hydrogen bonding (H-bonding) in a frequently used arylamide foldamer building block, *ortho*-methoxy-*N*-methylbenzamide. Our results show that solvents have a profound influence on the cumulative number and stabilizing effects of intramolecular H-bonds, and thus conformational preferences, of foldamers based on this compound. While intramolecular H-bonds are conserved in aprotic environments, they are significantly disrupted in protic solvents. Furthermore, these solvent effects can be accurately quantified using the computational approach presented here. The results could have significant implications in foldamer design, particularly for applications in aqueous environments.

### Introduction

Foldamers, synthetic oligomers that adopt defined, stable secondary structures in solution, have many realized and potential applications in a number of areas such as drug design and structural biology.<sup>1</sup> Aromatic oligoamides are among the most widely studied foldamers.<sup>2</sup> Their unique repetitive aromatic-amide pattern allows for structural predictability and tunability through the introduction of hydrogen bonds (H-bonds),  $\pi$ - $\pi$  stacking, and geometrical constraints into the molecular scaffold. H-bonds have a prominent place among the interactions employed in the foldamer design process, as they often provide a straightforward means of stabilizing defined conformations. For example, linear arylamide foldamers stabilized by H-bonds have been designed as bioactive peptide analogues, such as heparin antidotes<sup>3</sup> and amphiphiles with antimicrobial function.<sup>4</sup> Utilizing both intra- and intermolecular H-bonding, arylamide strands have also been designed to self-assemble into molecular duplexes which serve as recognition modules for the structured assembly of supramolecular entities, such as  $\beta$ -sheets and block copolymers.<sup>5</sup> Other motifs of aromatic oligoamide foldamers, such as macrocycles, hollow crescents, and helices, have also been obtained by designing backbones rigidified through intramolecular H-bonding.<sup>2b,5e,6–8</sup> Since most of the conceivable applications of foldamers will involve aqueous environments, it is important to address the influence of the solvent on H-bonding. As recently noted,<sup>2a</sup> systematic studies of the conformational preferences of foldamer building blocks at the atomic level are much needed. In this Letter, we analyze the intramolecular H-bonding behavior and related conformational preferences of a commonly used arylamide foldamer building block, and demonstrate that the effects of environments ranging

from protic to nonpolar can be accurately quantified by means of computational approaches.

One of the most frequently used monomers in aromatic oligoamides is *ortho*-methoxy-*N*-methylbenzamide (**1**, Figure 1a). On the basis of their relative positions, it is commonly assumed that an intramolecular H-bond will be present between the methoxy substituent and the N–H group of **1**. The design of various aromatic oligoamides, such as those mentioned above, relies on the presence of this intramolecular H-bond to stabilize desired conformations. As described herein, molecular dynamics (MD) simulations and nuclear Overhauser effect (NOE) NMR experiments carried out on **1** show that intramolecular H-bonds are lost to a significant extent in protic solvents (methanol, water) with respect to nonpolar environments (vacuum, chloroform).

### Results and Discussion

Our assessment of the effects of the intramolecular H-bonding on the conformational preference of **1** began with a systematic analysis of the torsional energy profiles around the C<sub>aromatic</sub>–C<sub>peptide</sub> (C<sub>a</sub>–C<sub>p</sub>) bond using *ab initio* methods.<sup>3b</sup> This study yielded torsional barriers for the C<sub>a</sub>–C<sub>p</sub> bond of 3.6 and 8.7 kcal/mol in *N*-methylbenzamide and **1**, respectively, reflecting the influence of intramolecular H-bonding. Using the general AMBER force field (GAFF)<sup>9</sup> modified according to these results and restrained electrostatic potential (RESP) charges,<sup>10</sup> we performed MD simulations of **1** in the gas phase, as well as in chloroform, methanol, and aqueous solutions. The C<sub>a</sub>–C<sub>a</sub>–C<sub>p</sub>–N dihedral angle distribution (Figures 1a and 2), intramolecular H-bonds (O $\cdots$ H–N), and intermolecular H-bonds (O $\cdots$ H–O<sub>solv</sub> and O<sub>solv</sub> $\cdots$ H–N) were analyzed. An O $\cdots$ H distance of less than 2.5 Å and an O $\cdots$ H–N or O $\cdots$ H–O angle larger than 120° were used as the criteria for the presence of H-bonds. It is also worth noting that, based on our analysis, C<sub>a</sub>–C<sub>a</sub>–C<sub>p</sub>–N angles within –50 to 50° are most suitable for the formation of the intramolecular H-bond.

\* To whom correspondence should be addressed. E-mail: v.pophri@usp.edu.

<sup>†</sup> University of the Sciences in Philadelphia.

<sup>‡</sup> Polymedix Inc.

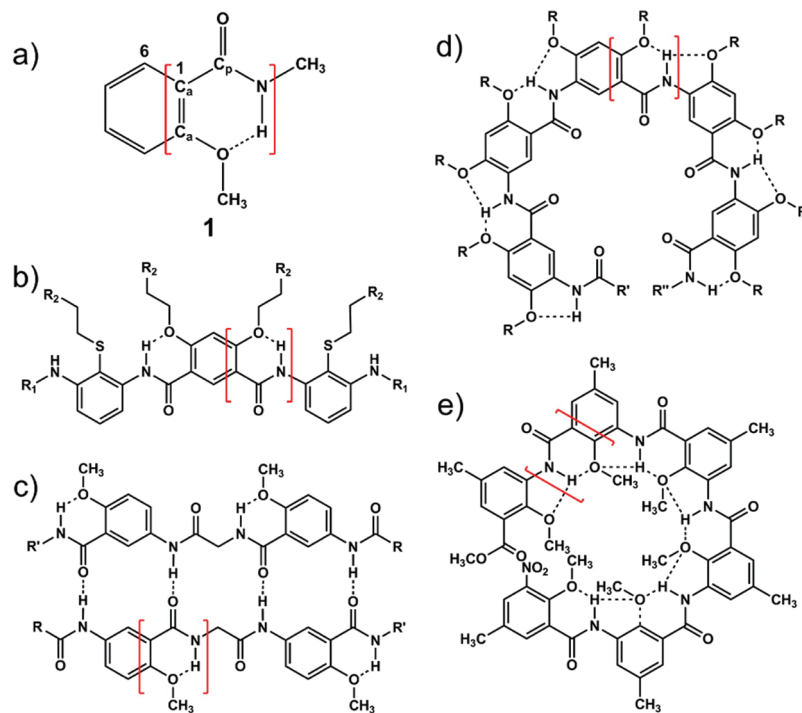


**Figure 1.** Structure, numbering, and dihedral angle definition for **1** (a). Intramolecular H-bond stabilized linear arylamide foldamer (b) designed as heparin antidote.<sup>3</sup> Molecular duplex (c) formed in  $\text{CHCl}_3$  by the self-assembly of two aromatic oligoamide strands through intermolecular H-bonds. Note that intramolecular H-bonds are introduced to preorganize individual strands for dimerization.<sup>5a</sup> Crescent-shaped (d)<sup>6a,b</sup> and “macrocyclic” (e)<sup>7</sup> aromatic oligoamide foldamers with the backbone rigidified by intramolecular H-bonding.

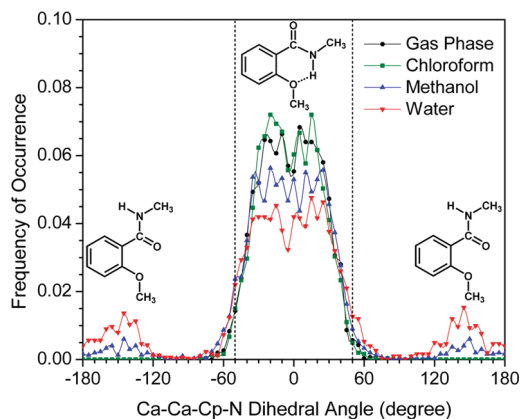


**Figure 2.** Distribution of the  $\text{C}_a\text{-C}_a\text{-C}_p\text{-N}$  dihedral angles from MD simulations of **1** in the gas phase, chloroform, methanol, and water.

As expected, simulations in the gas phase and in chloroform give virtually identical results. In both environments, the  $\text{C}_a\text{-C}_a\text{-C}_p\text{-N}$  dihedral distribution has one peak centered at  $0^\circ$ , with  $\sim 98\%$  of the rotamers within the  $-50$  to  $50^\circ$  region (Figure 2). Following the distance and angle criteria for H-bonding, about 80% of conformers exhibit intramolecular H-bonds. By slightly loosening the angle criterion to  $110^\circ$ , the percentage of H-bonded conformations increases to  $\sim 94\%$ , which is consistent with the dihedral angle distribution. Therefore, in the gas phase or nonpolar environment, compound **1** exhibits a persistent intramolecular H-bond between the methoxy and N-H groups.

The structures of the monomers are markedly different in methanol or water (Figure 2). The percentage of conformations within the  $-50$  to  $50^\circ$  dihedral region decreases from 98% in vacuum or chloroform to 88% in methanol and 74% in water. Both systems show peaks ranging from  $120$  to  $180^\circ$  and  $-180$  to  $-120^\circ$  in the  $\text{C}_a\text{-C}_a\text{-C}_p\text{-N}$  dihedral distribution, which give

rise to “reverse” conformations that make intramolecular H-bonds unlikely. H-bonding analysis gives similar results. Following the distance and angle criterion, the percentage of intramolecular H-bonded conformations falls from 80% in the gas phase or chloroform to 66% in methanol and 52% in water. Loosening the angle criterion to  $110^\circ$  increases the percentage of intramolecular H-bonded conformations in methanol and water to 80 and 61%, respectively, which are in line with the dihedral angle distribution.

The significant loss of intramolecular H-bonded conformations upon solvation is clearly due to competition between intramolecular H-bonding and formation of H-bonds with the protic solvents. Analysis shows that 18 and 44% of **1** exhibit intermolecular H-bonds of the  $\text{O}\cdots\text{H}-\text{O}_{\text{solv}}$  and/or  $\text{O}_{\text{solv}}\cdots\text{H}-\text{N}$  types in methanol and water, respectively. Furthermore, the majority of the “reverse” conformations form H-bonds with solvent molecules (60% in methanol and 80% in water). Figure 3 shows snapshots from the MD simulations in water depicting the “reverse” conformations and intermolecular H-bonds between **1** and solvent molecules. In addition, a much smaller but significant portion (14% in methanol and 32% in water) of the conformations within the  $-50$  to  $50^\circ$  window also forms intermolecular H-bonds with the solvent. Unlike the intramolecular H-bond case, loosening the angle criterion to  $110^\circ$  makes no significant changes in the intermolecular H-bonds analysis.

To corroborate the results from our computational studies, the conformational preferences of **1** in chloroform and both protic solvents were investigated using gradient-enhanced 1D-NOESY spectroscopy.<sup>11</sup> In chloroform, selective inversion of the N-H proton leads to an  $\sim 0.4\%$  enhancement of the methoxy signal (Figure 4a). Inversion of the N-H proton in methanolic solution causes a somewhat smaller NOE for the methoxy protons ( $\sim 0.3\%$ ), as well as a minor but detectable  $\sim 0.1\%$  enhancement of the H-6 aromatic proton signal (Figure 4b). In water, the same experiment leads to an  $\sim 0.3\%$  enhancement of

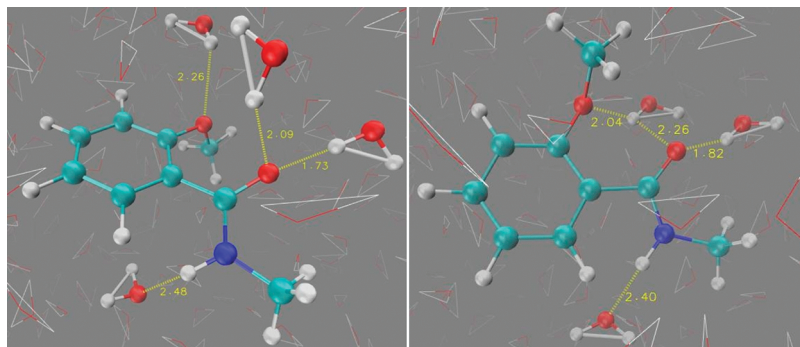


**Figure 3.** Snapshots from MD simulations of **1** in water showing the “reverse” conformations and intermolecular H-bonds to the solvent molecules. The dotted yellow lines indicate the locations of H-bonds and their lengths.

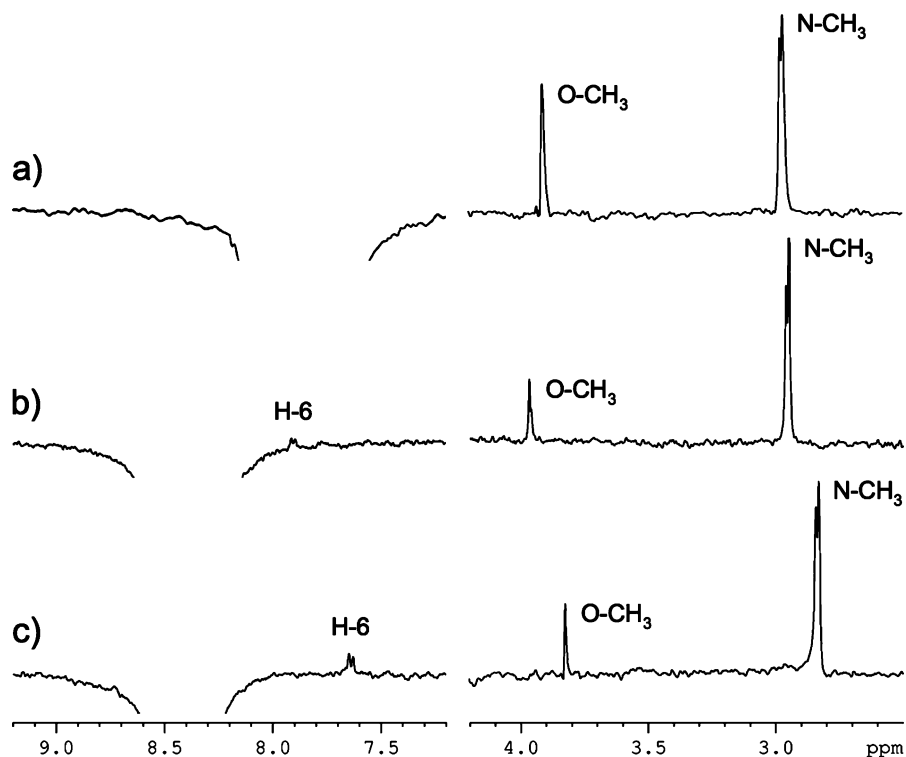


**Figure 4.** 1D-NOE spectra of **1** obtained upon inversion of the N–H resonance in chloroform (a), methanolic (b), and aqueous (c) solution. A mixing time of 600 ms was employed in all cases.

the methoxy signal, as well as to an  $\sim 0.4\%$  NOE for the H-6 proton (Figure 4c). These results confirm the presence of the “reverse” conformation predicted by our simulations in protic solvents. In particular, the progressive increase in the enhancement of the H-6 resonance and the concomitant decrease in the NOE of the methoxy signal observed when going from chloroform to water, clearly depicted in Figure 4, show that the “reverse” conformation becomes more populated in aqueous environments. The effective interproton distances<sup>12</sup> computed from the MD trajectories and NOE enhancements are also in good agreement. For example, the theoretical and experimental effective distances between the N–H and methoxy protons are 3.30 Å (MD) and 2.97–3.06 Å (NMR) in chloroform, 3.39 Å (MD) and 3.11–3.51 Å (NMR) in methanol, and 3.51 Å (MD) and 3.35–3.55 Å (NMR) in water. An analogous analysis yields effective distances between the N–H and H-6 protons of 4.35 Å (MD) in chloroform, which is consistent with the absence of an NOE between these protons in this solvent, 3.72 Å (MD) and 3.64–3.86 Å (NMR) in methanol, and 3.15 Å (MD) and 3.15–3.42 Å (NMR) in water.

Our combined computational and NMR study shows that the percentage of **1** retaining an intramolecularly H-bonded conformation decreases considerably in water. This finding could have significant implications in foldamer design, particularly for applications in aqueous environments. To illustrate this, we present here an example of how our approach can be used to rationalize an experimental observation. As reported by Gong and co-workers, the aromatic oligoamide strands shown in Figure 1c self-assemble into a duplex in chloroform, but not in water unless covalently cross-linked.<sup>13</sup> Our analysis of the conformational distribution of the strand obtained from MD simulations with optimized force field parameters<sup>3b</sup> can help explain this observation. Figure 5a shows that there are six backbone torsions governing the alignment of the four vectors defined by the N–H and C=O bonds ( $\mathbf{v}_1$ – $\mathbf{v}_4$ ). The  $\Phi/\Psi$  dihedral angle pair (blue) determines the alignment of  $\mathbf{v}_2$  versus  $\mathbf{v}_3$ , while the two arylamide dihedral angle pairs ( $C_a$ – $C_a$ – $N$ – $C_p$  (green)/ $C_a$ – $C_a$ – $C_p$ – $N$  (red)) determine the alignment of  $\mathbf{v}_1$  versus  $\mathbf{v}_2$  and  $\mathbf{v}_3$  versus  $\mathbf{v}_4$ . Their intervector angles  $\angle \mathbf{v}_1\mathbf{v}_2$  and  $\angle \mathbf{v}_3\mathbf{v}_4$  were calculated from the MD conformations and their



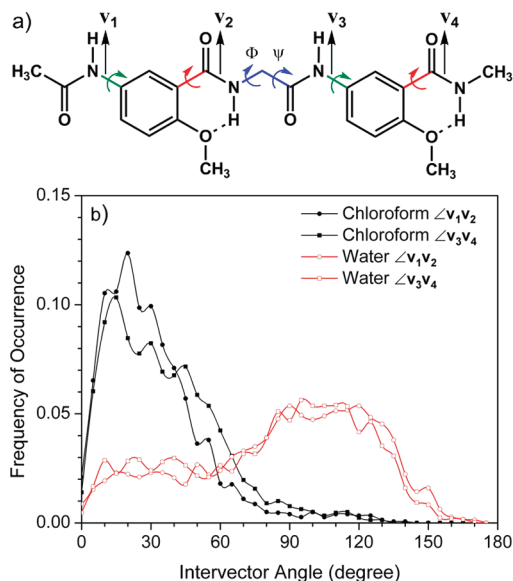


**Figure 5.** (a) Backbone torsions that govern the preorganization of the single aromatic oligoamide strand and definitions of the donor and acceptor vectors. (b) Distributions of intervector angles from the MD simulations in chloroform and water.

distributions analyzed (Figure 5b). In chloroform, the distribution of both angles peaks at  $< 90^\circ$ , indicating good alignments of  $v_1$  versus  $v_2$  and  $v_3$  versus  $v_4$ . In water, on the other hand, the distribution of both angles shifts largely to the antiparallel region ( $> 90^\circ$ ), indicating poor alignments of  $v_1$  versus  $v_2$  and  $v_3$  versus  $v_4$ . Analysis shows that the extensive loss of intramolecular H-bonds between the *ortho*-methoxy and amide groups contributes significantly to the antiparallel arrangement.

These results provide an atomistic explanation of the postulated duplex-forming mechanism.<sup>5,13</sup> In chloroform, the intramolecular H-bonds between the *ortho*-alkoxy and amide groups preorganize the arylamide strand, allowing complementary donor–acceptor patterns that lead to duplex formation. On the basis of our results, however, the probability of all intramolecular H-bonds being present simultaneously in aqueous solution would decrease as the number of monomers in the strand increases. This disrupts the preorganization and rigidity of the strand, and, together with nonspecific H-bonding with the solvent, hinders duplex formation. As stated earlier, foldamer conformation is controlled by a combination of structural features and noncovalent interactions, and a more comprehensive study of these effects is underway.

## Conclusions

In summary, we have shown that solvents have a profound effect on the cumulative number of intramolecular H-bonds, and thus conformational preferences, of foldamers based on **1**. Furthermore, this effect can be accurately quantified following the methodology presented here. As demonstrated above, MD simulations with properly adjusted force field parameters are indeed able to predict the conformational distribution of these molecules in various solvents. Since the design strategy, at least in a first approximation, relies on interactions between adjacent structural elements,<sup>2a,c</sup> this approach can be used as a critical

step in the arylamide foldamer design process prior to embarking on costly and time-consuming synthetic efforts.

**Acknowledgment.** The authors recognize the support from the KISK program, State of Pennsylvania, the NSF CCLI-A&I and MRI programs, Polymedix, Inc. (Z.L. and V.P.), and the Camille and Henry Dreyfus Foundation (R.C.R. and G.M.). We also thank Prof. Michael F. Bruist for his insightful comments and suggestions.

**Supporting Information Available:** Details of the synthesis of compound **1**, NMR and NOE data, simulation setup, and calculations of experimental and theoretical effective interproton distances. This material is available free of charge via the Internet at <http://pubs.acs.org>.

## References and Notes

- (1) (a) Gellman, S. H. *Acc. Chem. Res.* **1998**, *31*, 173–180. (b) Rowan, A. E.; Nolte, R. J. M. *Angew. Chem., Int. Ed.* **1998**, *37*, 63–68. (c) Hill, D. J.; Mio, M. J.; Prince, R. B.; Hughes, T. S.; Moore, J. S. *Chem. Rev.* **2001**, *101*, 3893–4011. (d) Cubberley, M. S.; Iverson, B. L. *Curr. Opin. Chem. Biol.* **2001**, *5*, 650–653. (e) Schmuck, C. *Angew. Chem., Int. Ed.* **2003**, *42*, 2448–2452.
- (2) (a) Huc, I. *Eur. J. Org. Chem.* **2004**, *1*, 7–29. (b) Li, Z.; Hou, J.; Li, C.; Yi, H. *Chem. Asian J.* **2006**, *1*, 766–778. (c) Goodman, C. M.; Choi, S.; Shandler, S.; DeGrado, W. F. *Nat. Chem. Biol.* **2007**, *3*, 252–262.
- (3) (a) Choi, S.; Clements, D. J.; Pophristic, V.; Ivanov, I.; Vemparala, S.; Bennett, J. S.; Klein, M. L.; Winkler, J. D.; DeGrado, W. E. *Angew. Chem., Int. Ed.* **2005**, *44*, 6685–6689. (b) Pophristic, V.; Vemparala, S.; Ivanov, I.; Liu, Z. W.; Klein, M. L.; DeGrado, W. F. *J. Phys. Chem. B* **2006**, *110*, 3517–3526.
- (4) Liu, D. H.; Choi, S.; Chen, B.; Doerksen, R. J.; Clements, D. J.; Winkler, J. D.; Klein, M. L.; DeGrado, W. F. *Angew. Chem., Int. Ed.* **2004**, *43*, 1158–1162.
- (5) (a) Gong, B.; Yan, Y. F.; Zeng, H. Q.; Skrzypczak-Jankun, E.; Kim, Y. W.; Zhu, J.; Ickes, H. *J. Am. Chem. Soc.* **1999**, *121*, 5607–5608. (b) Zeng, H. Q.; Miller, R. S.; Flowers, R. A.; Gong, B. *J. Am. Chem. Soc.* **2000**, *122*, 2635–2644. (c) Gong, B. *Synlett* **2001**, 582–589. (d) Zeng, H. Q.; Yang, X. W.; Flowers, R. A.; Gong, B. *J. Am. Chem. Soc.* **2002**, *124*, 2903–2910. (e) Sanford, A. R.; Yamato, K.; Yang, X. W.; Yuan, L. H.; Han, Y. H.; Gong, B. *Eur. J. Biochem.* **2004**, *271*, 1416–1425.
- (6) (a) Zhu, J.; Parra, R. D.; Zeng, H. Q.; Skrzypczak-Jankun, E.; Zeng, X. C.; Gong, B. *J. Am. Chem. Soc.* **2000**, *122*, 4219–4220. (b) Gong, B. *Chem.—Eur. J.* **2001**, *7*, 4336–4342. (c) Gong, B.; Zeng, H. Q.; Zhu, J.; Yuan, L. H.; Han, Y. H.; Cheng, S. Z.; Furukawa, M.; Parra, R. D.; Kovalevsky, A. Y.; Mills, J. L.; Skrzypczak-Jankun, E.; Martinovic, S.; Smith, R. D.; Zheng, C.; Szyperski, T.; Zeng, X. C. *Proc. Natl. Acad. Sci. U.S.A.* **2002**, *99*, 11583–11588. (d) Gong, B. *Acc. Chem. Res.* **2008**, *41*, 1376–1386.
- (7) (a) Yi, H. P.; Li, C.; Hou, J. L.; Jiang, X. K.; Li, Z. T. *Tetrahedron* **2005**, *61*, 7974–7980. (b) Li, Z.; Hou, J.; Li, C. *Acc. Chem. Res.* **2008**, *41*, 1343–1353.
- (8) (a) Berl, V.; Huc, I.; Khoury, R. G.; Krische, M. J.; Lehn, J. M. *Nature (London)* **2000**, *407*, 720–723. (b) Berl, V.; Huc, I.; Khoury, R. G.; Lehn, J. M. *Chem.—Eur. J.* **2001**, *7*, 2810–2820. (c) Berl, V.; Huc, I.; Khoury, R. G.; Lehn, J. M. *Chem.—Eur. J.* **2001**, *7*, 2798–2809. (d) Jiang, H.; Leger, J. M.; Huc, I. *J. Am. Chem. Soc.* **2003**, *125*, 3448–3449. (e) Jiang, H.; Leger, J. M.; Dolain, C.; Guionneau, P.; Huc, I. *Tetrahedron* **2003**, *59*, 8365–8374.
- (9) Wang, J. M.; Wolf, R. M.; Caldwell, J. W.; Kollman, P. A.; Case, D. A. *J. Comput. Chem.* **2004**, *25*, 1157–1174.
- (10) Bayly, C. I.; Cieplak, P.; Cornell, W. D.; Kollman, P. A. *J. Phys. Chem.* **1993**, *97*, 10269–10280.
- (11) Stott, K.; Keeler, J.; Van, Q. N.; Shaka, A. J. *J. Magn. Reson.* **1997**, *125*, 302–324.
- (12) Kessler, H.; Griesinger, C.; Lautz, J.; Muller, A.; van Gunsteren, W. F.; Berendsen, H. J. C. *J. Am. Chem. Soc.* **1988**, *110*, 3393–3396.
- (13) (a) Li, M.; Yamato, K.; Ferguson, J. S.; Gong, B. *J. Am. Chem. Soc.* **2006**, *128*, 12628–12629. (b) Li, M.; Yamato, K.; Ferguson, J. S.; Singarapu, K. K.; Szyperski, T.; Gong, B. *J. Am. Chem. Soc.* **2008**, *130*, 491–500.